Parametric fire design – zero-strength-layers and charring rates

Daniel Brandon, RISE Research Institutes of Sweden

Alar Just, RISE Research Institutes of Sweden

David Lange, RISE Research Institutes of Sweden

Mattia Tiso, Tallinn University of Technology

Keywords: Parametric fire, zero-strength-layer, charring rate

1 Introduction

In the field of fire safety engineering, performance based design methods are increasingly used to demonstrate that building designs are safe. However, performance based design is not commonly used for the design of timber structures, as there are not many relevant assessment methods available (Östman et al. 2010). For assessment whether the design of a building meets certain criteria, a design fire scenario is needed. Design fires often describe the temperature throughout a fire and are often based on dimensions, ventilation conditions and the fuel load of the compartment. Parametric fires are such design fires, used for structural calculations corresponding to ventilation controlled post-flashover fires in compartments, based on the compartment's dimensions, ventilation openings, lining materials, and the fuel load. Eurocode 1 (EN1991-1-2, 2004) includes parametric fires.

Annex A of Eurocode 5 (EN1995-1-2, 2004) offers a calculation method (the effective cross-section method) to determine charring rates of timber under parametric fire exposure of unprotected softwood only. However, Annex A is not accepted for use in all European countries, as the provided charring rates are questioned. Additionally, thicknesses for *zero-strength-layers* are missing, which take into account the strength reduction of uncharred but heated wood in the structural member. There is, furthermore, no distinction made between (1) a notional charring rate which accounts for increased charring around the corners of timber elements and (2) a one-dimensional charring rate.

As timber is combustible it contributes to the fuel load of a fire. If large surfaces of wood are exposed, its contribution should be included in the fuel load used to determine the parametric fire. It was previously shown that a relatively small amount of exposed timber, for example one wall of non-delaminating exposed timber in a compartment (Medina Hevia, 2014), does not significantly influence the temperature and fire duration of a compartment fire. This study focuses on parametric fires for compartments with a relatively small amount of exposed timber. The inclusion of the con-

tribution of large exposed timber surfaces to the fuel load is out of the scope of this paper and is studied in ongoing work. This paper presents an experimental and numerical study performed to determine one-dimensional charring rates, notional charring rates and zero-strength-layers corresponding to a range of parametric fire curves. The experimental and numerical studies are used as a benchmark for a proposed improvement of the effective cross-section method, which in 1995-1-2 (2004) is referred to as a reduced cross-section method.

2 Eurocode 1, Parametric fire exposure

Temperature curves for parametric fires were proposed by Wickström (1986) and were based on the standard fire and so called Swedish fire curves by Magnusson and Thelanderson (1970). The relationship between the fire temperature, *Θ*, and the time, *t*, is given by (EN 1991-1-2, 2002):

$$\Theta = 20 + 1325(1 - 0.324e^{-0.2t\cdot\Gamma} - 0.204e^{-1.7t\cdot\Gamma} - 0.472e^{-19t\cdot\Gamma} \quad (1)$$

where *Γ* is a factor that changes the heating rate corresponding to the thermal inertia of the compartment boundaries and the opening factor, *O*, of a compartment:

$$\Gamma = (O/\sqrt{pc\lambda})^2/(0.04/1160)^2 \quad (2)$$

Where, *p* is the density in kg/m3, *c* is the specific heat J/kgK and *λ* is the thermal conductivity in W/mK of the compartment's boundary.

The duration of the heating phase t_{max} (h) is related to the fuel load within the compartment:

$$t_{\max} = \max\left[(0.2\cdot 10^{-3} q_{t,d}/O); t_{\lim}\right] \quad (3)$$

Where: $q_{t,d}$ is the fuel load divided by the total surface area of the compartment boundaries (including walls and ceiling) in MJ/m^2; t_{lim} is the lower limit of the duration of the heating phase, which is 0:15h, 0:20h or 0:25h for slow, medium and fast fire growth, respectively. After the start of the cooling phase at t_{max}, the temperature decreases linearly until it reaches 20°C.

3 Eurocode 5, effective cross-section method

Eurocode 5 (EN 1995-1-2, 2004) provides an effective cross-section method for the assessment of structures exposed to fire. Following this method, a char layer and a so called zero-strength-layer on exposed sides of structural timber elements are subtracted from the original cross-section before the structural calculation is performed. The sum of the char layer thickness d_{char} and the zero strength layer thickness d_0 is termed the ineffective layer thickness d_{inef} (see Figure 1). As the strength of char is negligible in comparison with that of timber, charred material should be disregarded for the structural calculation. The zero-strength-layer compensates for heated but

uncharred timber and its thickness is dependent on the exposure. Eurocode 5, however, does not provide any information about the calculation of zero-strength-layer thickness corresponding to parametric fires.

Charring rates for parametric fires are provided in Annex A of EN 1995-1-2 (2004). The charring rates during the heating phase originate from Hadvig (1981):

$$\beta_{par} = 1.5\beta_n \frac{0.2\sqrt{\Gamma} - 0.04}{0.16\sqrt{\Gamma} + 0.08} \quad (4)$$

where, β_n is the notional charring rate (mm/min)

For a duration of t_0, which is shorter than the duration of the heating phase, the charring rate for parametric fires, β_{par}, is taken into account. The charring rate for the cooling phase, linearly decreases to zero for a duration equal to two times t_0 (see Figure 1, right). The charring depth at any time can then be calculated from the integral of the charring rate function shown in the figure.

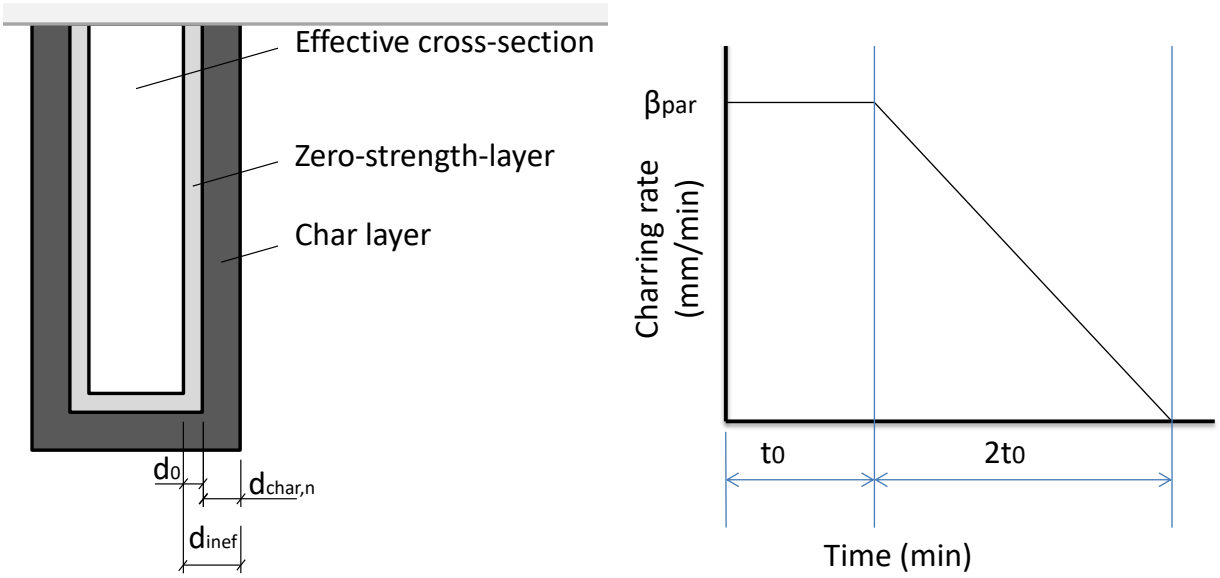

Figure 1: Char layer and zero-strength-layer of a beam cross-section exposed on three sides (left) and charring rate during the heating and cooling phases (right)

4 Experimental study

The number of parametric fire test results available is very limited. Therefore, two test series have, recently, been performed of which the second series (Series B) is also discussed by Lange et al. (2015). The tests of the two series were exposed to, in total, five different parametric fires in agreement with Eurocode 1, EN1991-1-2 (2002). The implemented fires were within a range that is relevant for under ventilated compartment fires.

Test series A comprised of model scale furnace tests and consisted of less specimens than test series B. However, due to the smaller scale it was possible to perform tem-

perature measurements at a large number of positions in each beam. Test series A is, therefore, used to set up a numerical method to predict material temperatures.

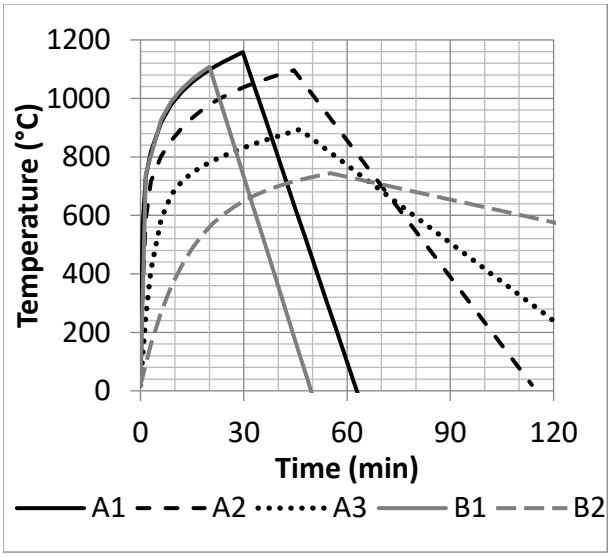

Table 1. Parameters of tested fire curves

Name	Fuel load density $q_f(q_{td})$ (MJ/m^2)	Thermal inertia (J/m^{2}s$^{1/2}$K)	Opening factor (m$^{1/2}$)	Heating rate factor
A1	675(149)	600	0.06	8.41
A2	675(149)	600	0.04	3.74
A3	675(149)	350	0.02	0.93
B1	250(92)	1160	0.12	9.00*
B2	250(92)	0.02	0.02	0.25*

*Figure 2: Parametric temperature curves *medium fire growth rate*

4.1 Setup of test series A (model scale tests)

Ten glued laminated timber beams were exposed to parametric fires (A1 to A3) in a fire testing furnace. The series comprised of six 4-point bending tests of strength graded glued laminated beams (see Figure 3) and four unloaded tests of glued laminated beams with cross-sections of 180x260mm. The loads were chosen so that the two specimens tested under the same parametric fire exposure failed at different times during the cooling phase. The time to failure and the deflection of the beam was recorded. For all tests, the charring rates were determined in horizontal and vertical directions using three thermocouple series of 10 thermocouples for each specimen positioned in the timber. Figure 3 shows the positions of one of those sets.

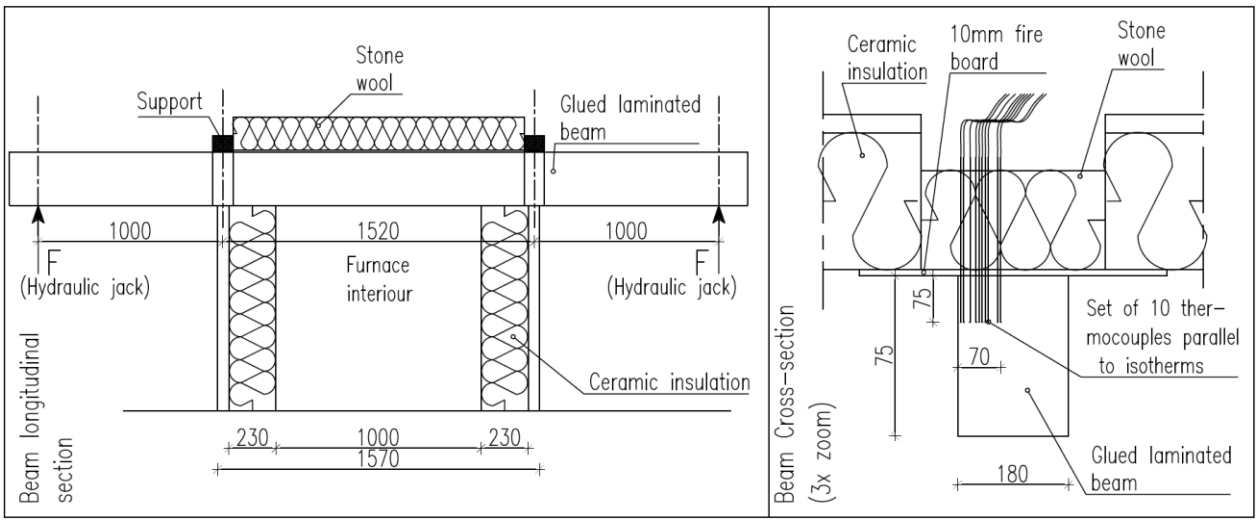

Figure 3: Longitudinal section (left) and cross-section (right) of a glued laminated beam in a four-point bending test on top of a model-scale furnace

In order to assess the validity of structural calculations of fire exposed timber, its strength at ambient conditions should be known. Therefore, glued laminated beam specimens were made of lamellas that were strength graded in accordance with Olsson and Oscarsson (2016). Out of 105 strength graded lamellas, eight beams were glued using six lamellas that had similar estimated strengths, with less than 1N/mm^2 difference between the strongest and weakest lamella in one beam. The average moisture content of all lamellas was 12.0% with a standard deviation of 0.4%.

4.2 Setup of test series B (full scale tests)

This series of 4 tests was based on EN 1363-1 and EN 1365-3, with 2 significant deviations. Firstly, 2 of the tests used the standard fire temperature-time curve, whereas the other two tests used temperature-time curves based on the parametric fire model of EN 1991-1-2 (2002), with two different opening factors. Secondly, for the entire series the beams spanned the short axis of a 3 m x 5 m horizontal furnace, with a distance between the supports of 3300 mm (see Figure 4). This meant that 8 glulam beams with cross-section 139 mm x 269 mm could be tested in each test. The beams in 3 of the 4 tests were subjected to 4 point bending, with different loads applied to the beams in pairs. The loads were chosen to encourage failure at different times during the fire tests. As the beams failed, the hydraulic loading cylinders were retracted and any openings in the top of the furnace were sealed with mineral wool. At the end of the tests, all of the beams were removed from the furnace as quickly as possible, burning was extinguished and the char layer was mechanically removed.

45 beams were divided into 5 groups (4 groups of 8, and 1 of 10- leaving 3 spare) using a dynamic estimate of their stiffness. Each group had a very similar mean and standard deviation in stiffness. The group of 10 was then subject to static testing until failure, with the assumption that the distribution of strength and stiffness of this group was the same as the four to be used in the fire tests. During the fire test, various measurements were taken, including deflection and temperatures in the cross-section. A detailed sectional analysis was also carried out after the tests.

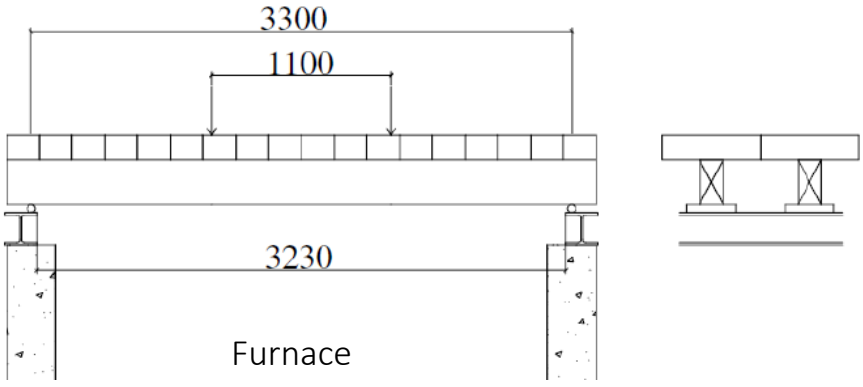

Figure 4: Setup of a four-point bending test on top of a full-scale furnace

5 Numerical analysis

A combination of a numerical heat transfer analysis for calculation of material temperatures in a large number of locations (step 1) and a numerical structural analysis to determine the structural capacity based on temperatures calculated in step 1 (step 2) is performed. For the structural calculation in step 2, a reduction of tensile and compressive strength (f_t and f_c) and tensile and compressive Young's modulus (E_t and E_c) is based on temperatures as shown in Figure 5 (König and Walleij, 2000).

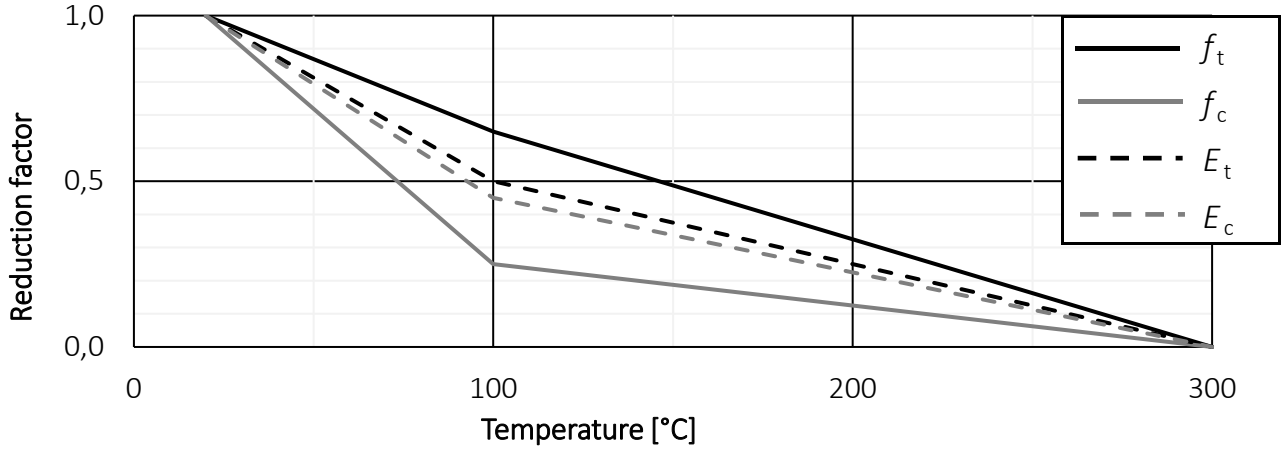

Figure 5. Temperature dependent reduction factors for strength and Young's modulus

The heat transfer analysis of step 1 is performed using a set of thermal properties that is effective to calculate temperatures within timber elements for the full duration of a parametric fire assuming solely conductive, radiative and convective heat transfer. Additionally, it is assumed that the heat source is in the compartment and not within the surface of the timber, as done in multiple previous studies (e.g. König and Walleij, 2000). In reality, mass transfer (moisture and gasses), fissures in the char layer and oxidation have an influence on the temperature development in timber exposed to fires. Due to the simplifications it is not possible to have a single set of thermal properties that is effective to predict temperatures in timber exposed to all possible parametric fires (Hopkin et al. 2011).

5.1.1 Thermal simulations of experiments

In this section sets of thermal properties are presented that result in accurate temperature predictions in the heating phase as well as the cooling phase. Although, it is recognized that changes of thermal properties are mostly irreversible in a fire (for example, char does not turn back to timber), it is assumed that these properties are reversible. This assumption allows the search for effective thermal properties that are effective in, both, the heating and the cooling phase of a fire.

Using computer algorithm by Mäger et al. (2016) and numerical temperature calculations performed with SAFIR 2007, the set of thermal properties shown in Table 2 was obtained. The used convection coefficient and emissivity are 25 W/m^{2}K and 0.8, respectively, which are in accordance with EN 1991-1-2 (2002) and EN 1994-1-2 (2004).

In order to have one framework that fits a range of parametric fires, the thermal conductivity corresponding to temperatures of 250°C and higher are multiplied by a factor, α. α was determined for three tests corresponding to different heating rates, Γ, and results are shown in Table 2. The thermal properties can be obtained by linear interpolation with respect to temperature. In order to demonstrate the validity of the framework the predicted and the experimentally determined temperature distributions corresponding to fire curves A1 to A3 are given in Figure 6 and Figure 7. Good agreement was seen between the calculated and measured internal temperatures.

Table 2. Temperature and effective thermal properties

Temperature (°C)	Thermal conductivity (W/mK)	Specific heat (J/kgK)	Density (kg/m^3)
20	0.12	1530	495
98	0.133	1770	495
99	0.265	13600	495
120	0.272	13500	495
121	0.137	2120	495
200	0.150	2000	495
250	0.136 x α*	3337	460
300	0.106 x α*	1463	257
350	0.077 x α*	1751	188
400	0.084 x α*	2060	163
500	0.099 x α*	2472	155
600	0.194 x α*	2884	139
800	0.385 x α*	3399	129
1200	1.65 x α*	3399	0

*α that results in the best fit with experimental data is determined for three tests of series A.

**ω is the initial moisture content

Table 3. α for different heating rates

Parametric fire	Heating rate factor Γ	α
A1	8.41	1
A2	3.74	1.1
A3	0.93	1.35

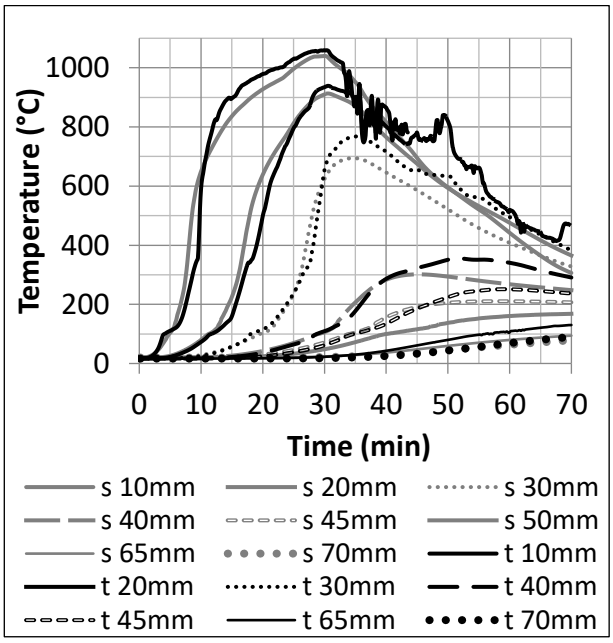

Figure 6. Numerical and experimentally determined temperatures at different depths. Parametric curve A1

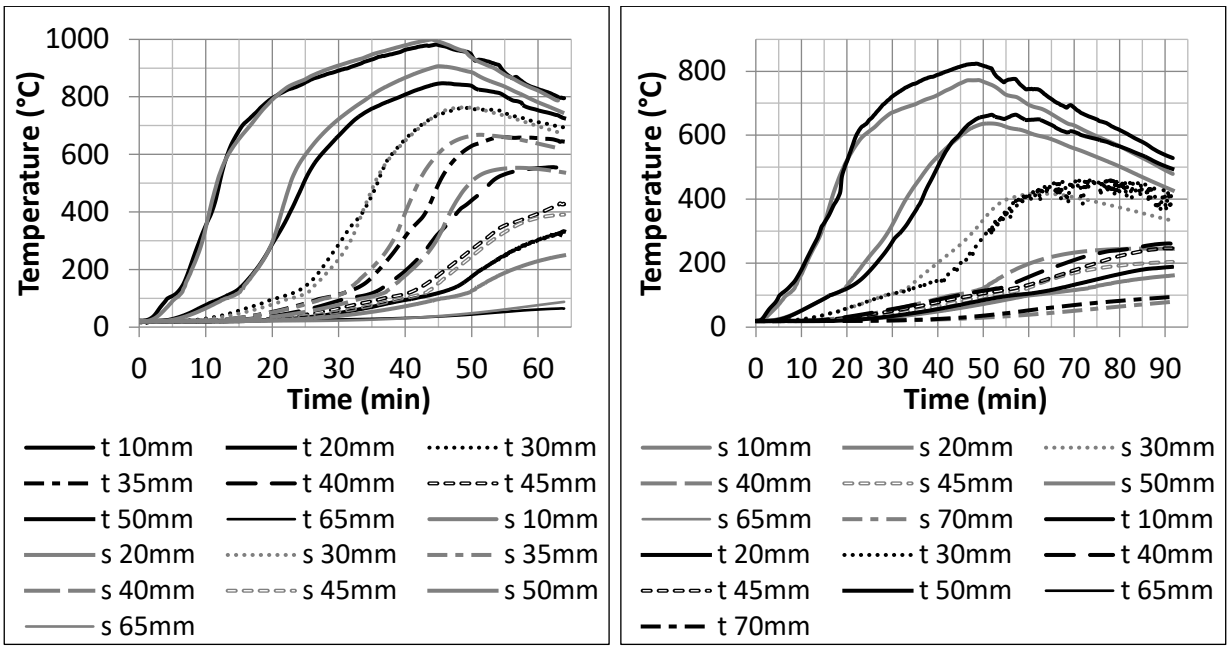

Figure 7. Numerical and experimentally determined temperatures at different depths. Parametric curve A2 (left) A3 (right)

For the heat transfer model (step 1 of the analysis) a symmetrical half of the beams cross-section (180/2 x 260mm) was discretised using square elements of 1x1mm. The two exposed sides of the symmetrical half were subjected to the parametric temperature curves, assuming the same convection and emissivity as mentioned before. There was no heat transfer on the other sides, to simulate a symmetry plane and the unexposed side of the beam. The average temperature (of four nodes) of every element was calculated and a numerical calculation according to Schmid and König (2010) with the same element mesh using the reduction coefficients of Figure 5 was performed, to determined the moment capacity of the heated beam.

6 Generation of a new effective cross-section method for parametric fires

For application of the effective cross-section method to calculate the structural capacity of timber members exposed to fire, charring rates and the zero-strength-layer are necessary input parameters. In the standard ISO 834 fire, the zero-strength-layer can be taken as constant after 20 minutes according to Eurocode 5. In the cooling phase of a parametric fire, the correlation between the charring rate and the reduction of load bearing capacity is not as straightforward. The charring rate will decrease and charring can completely stop during the cooling phase. However, after the charring has stopped the capacity of the beam continues to decrease. In the numerical model, the end of charring is taken as the time at which the 300°C isotherm stops to advance. After that, internal material with temperatures lower than 300°C continues to heat up as a result of diffusion from the hotter char layer, meaning that the load bearing capacity of the cross-section still reduces as the thickness of the temperature

affected timber increases. The zero-strength-layer is, therefore, not constant in the cooling phase. Consequently, predictions of the real charring rate in the cooling phase are not practical, as its use for calculations only complexifies the calculation of the thickness of the zero-strength layer. Instead, an effective charring rate is introduced so that a constant zero-strength-layer can be assumed. The zero-strength-layer is dependent on the heating rate, Γ.

The numerical model was used to predict the width of the ineffective layer, d_{inef}, that should be subtracted from the initial cross-section to calculate the load bearing capacity for the full duration of the fire. The thickness of this layer can be obtained by solving the following equation to d_{inef}.

$$W_{ef} = \frac{(b-2d_{inef})(h-d_{inef})^2}{6} = \frac{M_{ult}}{f_b} \quad (5)$$

where: W_{ef} is the effective section modulus; M_{ult} is the failure load; b is the initial beam width; h is the initial beam depth; f_b is the estimated bending strength of the beam.

The thickness of the zero-strength-layer can be estimated by solving the following equation to d_0:

$$W_{300} = \frac{(b-2(d_{inef}-d_0))(h-d_{inef}+d_0)^2}{6} \quad (6)$$

where: W_{300} is the section modulus of the part of the cross-section with temperatures lower than 300°C, which can be based on heat transfer analyses. The zero-strength-layer corresponding to the start time of the cooling phase is determined numerically for parametric fires A1, A2 and A3. It should be noted that the zero-strength-layer is approximately, but not exactly constant. The following empirical equation is proposed for the heating rate dependence of the zero-strength layer:

$$d_0 = 8.0 + 0.02\Gamma - 0.05\Gamma^2 \quad (7)$$

In Section 7 the extrapolation of the above equation is tested for heating rate factors of 0.25 and 9.0. Care should be taken to extrapolate the function any further as it is an empirical relationship.

The charring rate during the heating phase is based on the series of experimental results. The charring rates where determined from the location and time at which the last thermocouple of one thermocouple series reached 300°C. To avoid unreliably results, only thermocouples that were positioned parallel to the isotherms, in agreement with Annex C of EN 1363-1 (2012), were used for determining the charring rate. Additionally, experimental results of test series B1 were not included as none of the thermocouple readings exceeded 300°C during the heating phase. The following equation is proposed for the one dimensional charring rates corresponding to different fire heating rates: $\beta_{par;0} = \beta_0 \Gamma^{0.28}$ (8)

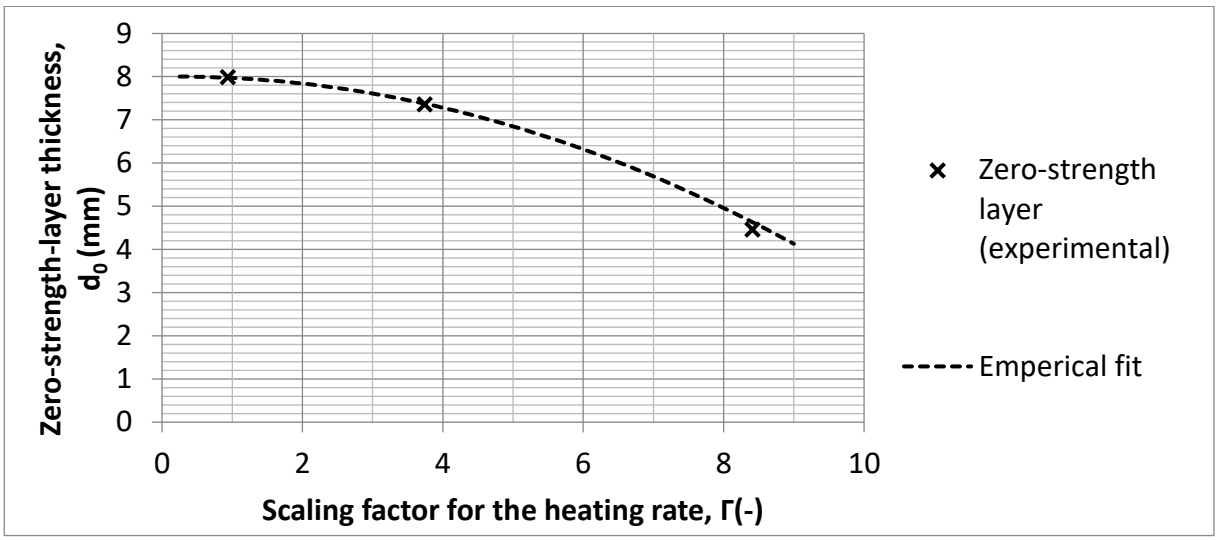

Figure 8. Relationship between Γ and zero-strength-layer (numerical)

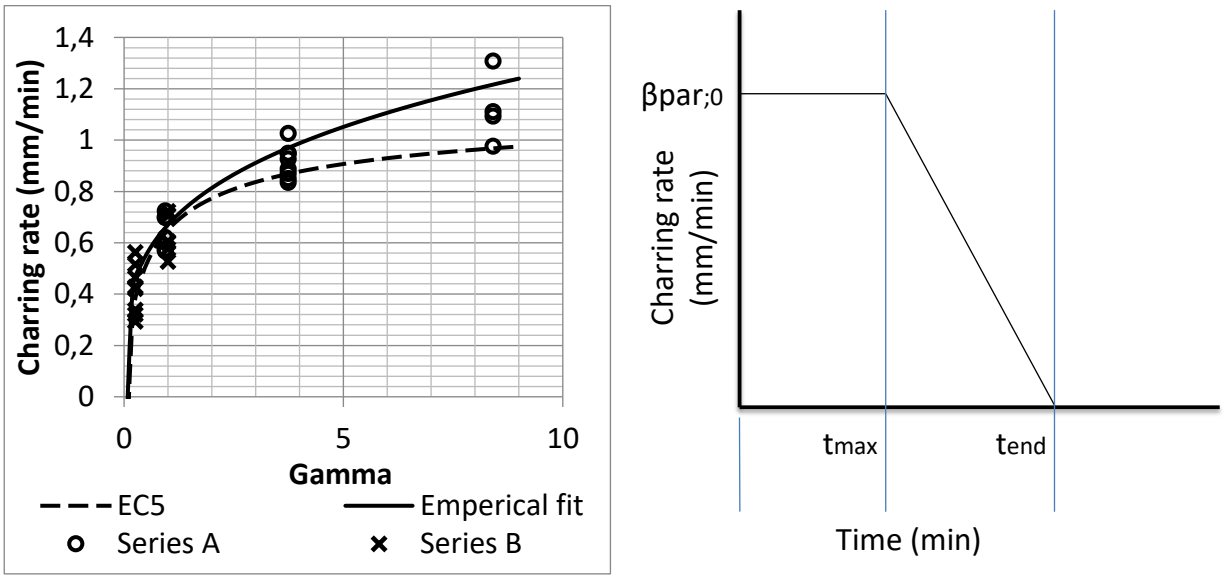

Figure 9. Relationship between Γ and the one-dimensional charring rate(left) proposed effective charring model (right)

An effective charring model is proposed with significant differences from the current charring model in EN1995-1-2 (2004). In the proposed model the charring rate is constant for the entire heating phase. It should be noted that t_0 of the Eurocode 5 model is not equal to the duration of the heating phase, t_{max}. t_{end} is the time at which the temperature of the parametric fire curve returns back to 20°C:

$$t_{end} = \frac{625 t_{\max} x \cdot \Gamma + \Theta_{\max} - 20}{625 \cdot \Gamma} \quad \text{if} \quad t_{\max} \cdot \Gamma \le 0.5 \qquad (9)$$

$$t_{end} = \frac{-250 t_{\max}^2 x \cdot \Gamma^2 + 750 t_{\max} x \cdot \Gamma + \Theta_{\max} - 20}{250 \cdot \Gamma (t_{\max} \cdot \Gamma - 3)} \quad \text{if} \quad 0.5 < t_{\max} \cdot \Gamma < 2 \qquad (10)$$

$$t_{end} = \frac{250 t_{\max} x \cdot \Gamma + \Theta_{\max} - 20}{250 \cdot \Gamma} \quad \text{if} \quad t_{\max} \cdot \Gamma \ge 2 \qquad (11)$$

The maximum fire temperature Θ_{max} can be obtained by substituting t_{max} for t in Eq.(1). The effective charring depth, $d_{char;ef,}$ at any time can be calculated using:

$$\beta_{par;eff} = k_{char}\beta_{par;0} \quad (12)$$

$$d_{char;eff} = \beta_{par;ef}\, t \quad \text{for } t \le t_{\max} \quad (13)$$

$$d_{char;ef} = \beta_{par;ef} t_{\max} + 0.5 * \left(\frac{-\beta_{par;ef}}{t_{end} - t_{\max}} \right) \cdot (t - t_{\max})^2 + \beta_{par;ef} (t_{end} - t_{\max}) \quad \text{for } t > t_{\max} \quad (14)$$

Where k_{char} is a factor that accounts for corner roundings and is the ratio between the one-dimensional charring depth and the notional charring depth.

The notional charring rate at the end of the heating phase was estimated from the numerical study:

$$\beta_{par;n} = \frac{d_{inef} - d_0}{t} \quad (15)$$

The one-dimensional charring rate was determined from a one dimensional heat transfer model using the same thermal properties and fire exposure. The ratios between the average notional and one-dimensional charring rates at the end of the heating phase were 1.10, 1.03 and 1.12 for parametric fires A1, A2 and A3, respectively. A ratio of k_{char}=1.1 corresponds well with the numerical results and is approximately similar to the ratio between the one-dimensional and notional charring rates according to EN1995-1-2 (2004). This ratio is used for predictions discussed further in this paper.

In the next section, the validity of the proposed effective cross-section method applied to parametric fires is assessed using comparisons with experimental and numerical results.

7 Assessment of the new effective cross-section method

The effective cross-section method proposed in Section 6 is assessed using results of the experimental and numerical studies discussed in Section 4 and 5. Numerically and experimentally determined thicknesses of the ineffective layer, $d_{inef,}$ together with predictions using the proposed effective cross-section method for parametric fire curves A1, A2, A3, B1 and B2 (see Table 1) are given in Figure 10 and Figure 11. Additionally, predictions of the charring depth according to the Eurocode are given.

It can be seen that the numerically predicted charring depth and the effective depth deviate significantly in the cooling phase of the fire. The charring rate prediction of EN 1995-1-2 (2004) is based on experimental results (Hadvig, 1981) and shows good agreement with the numerical predictions. The effective char depth according to the

proposed model deviates significantly from predicted charring rates. However, it seems effective to predict the ineffective depth using only a constant zero-strength-layer, because the predicted ineffective depth corresponds well with the numerical and experimental results. The ineffective depth corresponding to experiments is calculated and is defined as the ineffective depth that leads to failure of the beam, using the predicted strength properties of the beam.

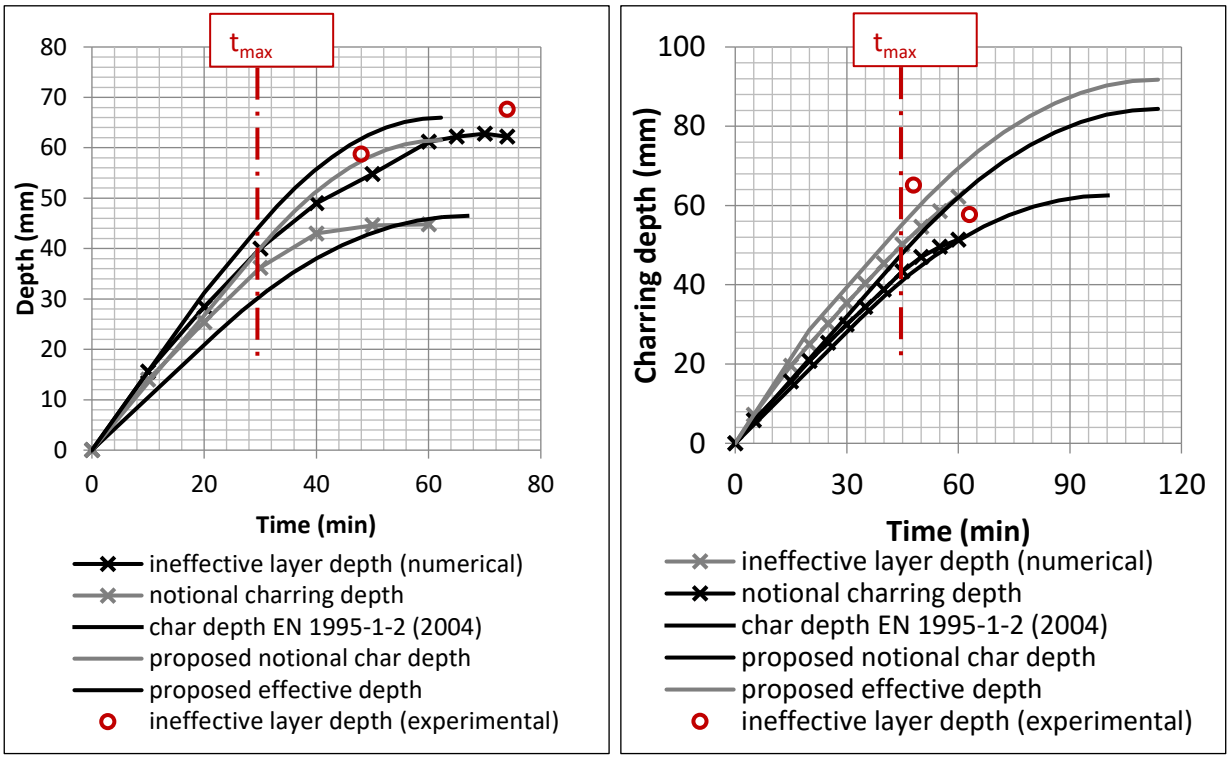

Figure 10. Numerical, analytical predictions of the charring depth, d_{char}, and ineffective depth, d_{inef}, and experimental results. Parametric fire A1 (left) and A2 (right)

Figure 12 shows comparisons between the experimental and predicted load bearing of glued laminated beams exposed to parametric fires, at the time of failure. Predictions were made using the proposed model and the current model of EN1995-1-2 (2004). For the latter, a zero-strength-layer of 7mm was taken for all fire exposures irrespective of the heating rate, as there is no zero-strength-layer specified for parametric fires. It can be seen that the calculated load bearing capacity using the proposed approach is generally more similar to the tested load bearing capacity. The current calculation method of EN1995-1-2 (2004) generally leads to unsafe predictions, indicating that the model should be updated in the next version of Eurocode 5.

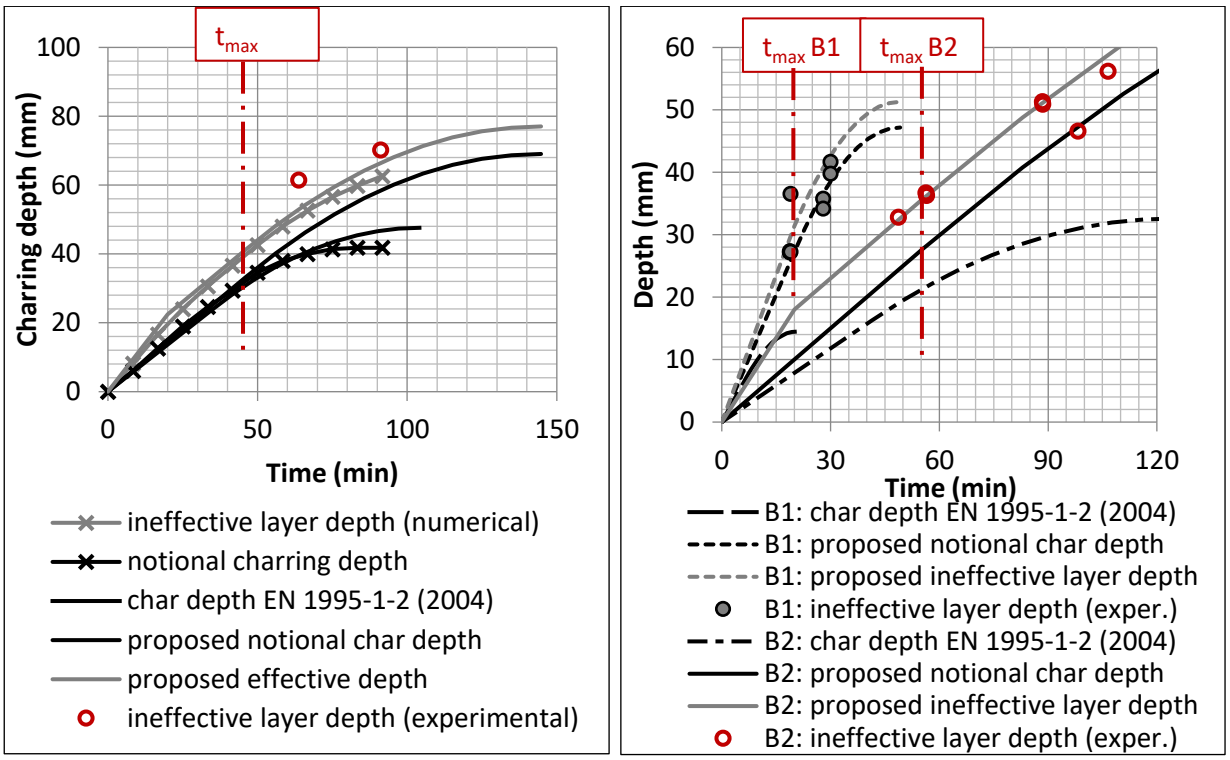

Figure 11. Numerical, analytical predictions of the charring depth, d_{char}, ineffective depth, d_{ineff}, and experimental results. Parametric fire A3 (left) B1 and B2 (right)

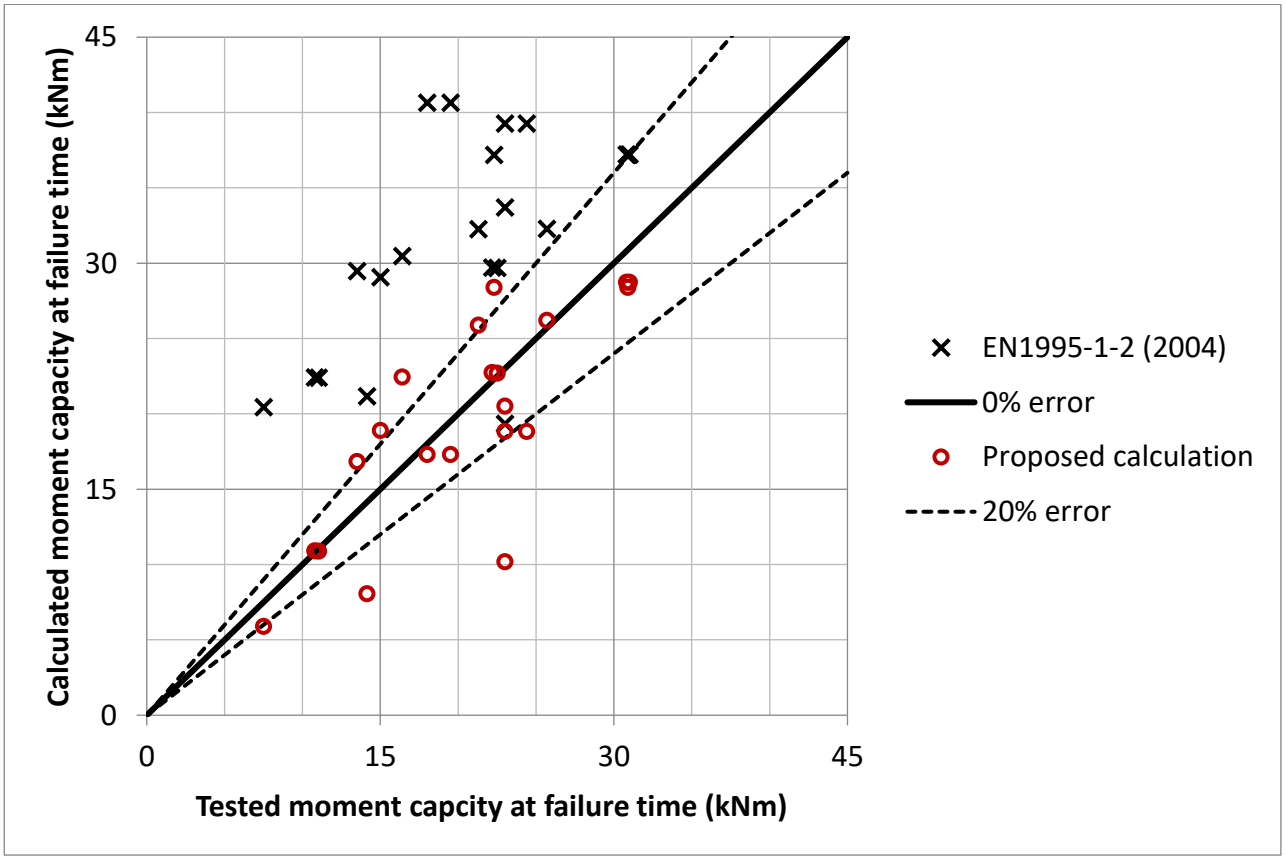

Figure 12. Calculated versus tested moment capacity at failure time

8 Conclusions

A new effective cross-section method for predictions of structural failure of timber exposed to parametric fires is proposed. Comparisons with experimental and numerical results showed that the current method given in EN1995-1-2 (2004) is unconservative and that the proposed model predicts structural failure more accurately.

References

EN1363-1 (2012). Fire resistance tests. General requirements. CEN, Brussels.

EN1995-1-2 (2004). Eurocode 5: Design of timber structures - Part 1-2: General - Structural fire design. CEN, Brussels.

EN1991-1-2 (2002) Eurocode 1: Actions on structures - Part 1-2: General actions - Actions on structures exposed to fire. CEN, Brussels.

Hadvig S. (1981). Charring of wood in building fires. Technical University of Denmark, ISBN 87-87 245-83-3.

Hopkin, D., El-Rimawi, J., Silberschmidt, V., and Lennon, T. (2011) An effective thermal property framework for softwood in parametric design fires. Journal of Construction & Building Materials 25(5), pp 2584-2595.

König J., Walleij L. (2000) Timber frame assemblies exposed to standard and parametric fires, Part 2. Institutet för träteknisk forskning, Stockholm, Sweden.

Lange D., Boström L., Schmid J., Albrektsson J. (2015) The reduced cross section method applied to glulam timber exposed to non-standard fire curves. Fire Technology DOI: 10.1007/s10694-015-0485-y

Mäger K.N., Brandon D., Just A. (2016) Determination of the effective thermal properties for thermal simulations. in: Proceedings of INTER, Graz, Austria.

Magnusson S.E., Thelanderson S. (1970) Temperature-time curves of complete process of fire development. *Acta Polytechnica Scandinavica,* 65.

Medina Hevia A.R. (2014). *Fire resistance of partially protected cross-laminated timber rooms*. Master thesis. Department of Civil and Environmental Engineering Carleton University, Ottawa, Ontario, Canada.

Olsson A. and Oscarsson J. (2016) Strength grading on the basis of high resolution laser scanning and dynamic excitation. *Eur. J. Wood Prod*.

Östman et al. (2010). Fire safety in timber buildings. Technical guideline for Europe. SP Technical Research Institute of Sweden, SP-Report 2010:19. Stockholm, Sweden.

Schmid J., König J., Köhler J. (2010) Fire exposed cross-laminated timber–modelling and tests. In: World conference on timber Engineering 2010. Riva del Garda, Italy.

Wickström U. (1986). *Application of the standard fire curve for expressing natural fires for design purposes*. Fire Safety: Science and Engineering, ASTM STP 882